PHILOSOPHICAL TRANSACTIONS OF THE ROYAL SOCIETY A MATHEMATICAL, PHYSICAL & ENGINEERING SCIENCES

Quartz Fibre Accelerometers

B. Block and J. Dratler

Phil. Trans. R. Soc. Lond. A 1973 **274**, 231-243
doi: 10.1098/rsta.1973.0048

Phil. Trans. R. Soc. Lond. A. **274**, 231–243 (1973) [231]
Printed in Great Britain

Quartz fibre accelerometers

By B. Block and J. Dratler, Jr†
Institute of Geophysics and Planetary Physics, University of California at San Diego, California, U.S.A.

New vertical and horizontal accelerometers based on torsion fibres of fused quartz and differential capacitance position sensors are discussed. The instruments have low drift, flat response from d.c. to nearly 1 Hz, and gain sufficient to measure tidal and seismic accelerations. They are small, weigh less than 9 kg, and have strict control of internal temperature and pressure.

Tidal, free oscillation, and seismic data from the accelerometers are presented. Records of earthquakes of surface wave magnitude 6.5 to 7.5 yield free oscillation spectra with greater than 20 dB signal-to-noise ratio. Records of distant teleseisms provide a detection threshold of surface wave magnitude 2.5 at a distance of 30°. A record of the San Fernando earthquake of February 1971 gives an upper bound of 1mm for a vertical displacement step 190 km from the source.

Introduction

Torsion fibres have been used in measuring instruments for nearly two centuries. In 1798 Cavendish constructed a torsion balance to weigh the earth. By the beginning of this century, the excellent properties of fused quartz fibres for sensitive measurement were well known, as evidenced by an interesting review by Boys (1923). More recently, Roll, Krotkov & Dicke (1964) used a torsion meter based on a long quartz fibre to repeat the Eötvös experiment, showing the equivalence of inertial and passive gravitational mass with great precision.

The major advantage of torsion fibres for sensitive measurement lies in the provision of very small, but reliable, restoring forces. In accelerometers, such small restoring forces allow high sensitivity to be achieved without the use of large inertial masses. Fused quartz torsion fibres in the present instruments provide free periods near 1 s with masses of about 10 g. With such small masses, the Q of the mechanical system must be kept high to reduce the Brownian noise. The values of Q for the present instruments are 20 or greater.

Another advantage of torsion fibres, as opposed to springs, levers or strip supports, is their high degree of symmetry, which allows them to approach the ideal of a single degree of freedom. In the present instruments, both high fibre tension, about 1 kg mass, and magnetic eddy current damping help prevent cross-coupling of vibrational energy to the measuring mode. The fringe fields from the damping magnets determine the Q of the measuring mode. The advantage of fused quartz, or vitreous silica, as the fibre material lies in its long-term elastic stability under stress.

The accelerometers

The vertical quartz fibre accelerometer (Block & Moore 1970; Dratler 1971; Block & Dratler 1972), whose mechanical system is shown in figure 1, was developed over a period of 5 years by Block and Moore. Its inertial mass is a flat plate supported in a horizontal plane by torsion in the fibre. The fibre itself is drawn from a thick matrix rod of fused quartz. Two active torsion sections of small diameter lie between ground clamping flats, which permit drift-free mounting of the fibre and mass. The instrument frame shown in the drawing is about 11.5 cm in height.

† Present address: DIAX, Inc. Box 2207, La Jolla, California 92037, U.S.A.

The mechanical system for the horizontal accelerometer (Dratler 1971; Dratler & Block 1972), developed by the present authors, is shown in figure 2. In essence, it is a simple pendulum using the fibre as a stable pivot. When the pendulum is displaced a small amount from the vertical, less than 1.5 % of the restoring force is supplied by the fibre torsion. The rest is supplied by gravity. The length of the pendulum is 25 cm.

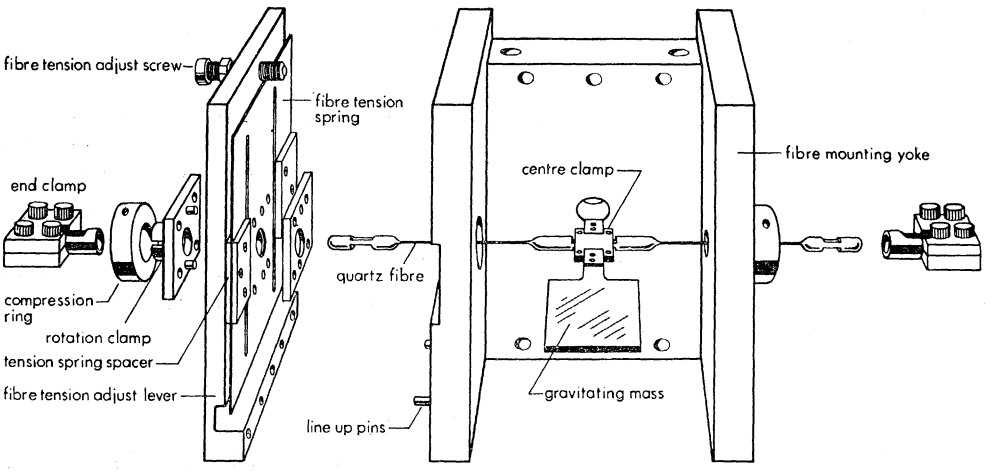

FIGURE 1. Mass–fibre system for vertical accelerometer. Mass is held in horizontal plane by torsion in two active sections of fibre. Note centre clamping section of matrix rod between active sections. Plate at left is part of tensioning mechanism. Height of frame is 11.5 cm.

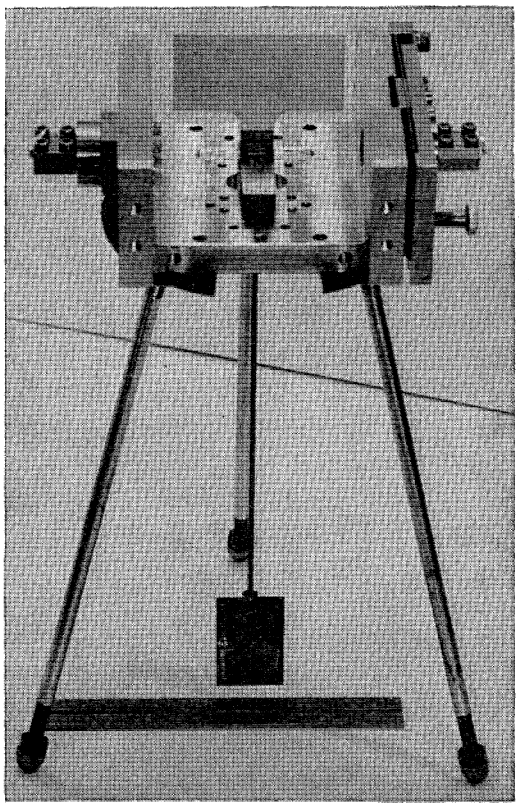

FIGURE 2. Pendulum assembly for horizontal accelerometer. Plate at bottom is pendulum mass. Large plate at top is centre element of transducer, while small fin is used for eddy current damping of unwanted modes of vibration.

Both the vertical and horizontal accelerometers use a differential capacitance position sensor as the transducer. This device consists of three parallel plates, the centre of which is the moving element. The configuration used here is quite similar to that described by R. V. Allen in another article in this volume and will not be described in detail. The advantages of such a sensor are finite response at d.c., good linearity, high sensitivity, and small size. If fringing fields are neglected and a high impedance preamplifier is used, the output of the sensor is strictly linear over the full range of mechanical motion. In conjunction with the commercial preamplifier and phase sensitive detector, this transducer can detect a displacement of 5 pm in a 1 s averaging time.

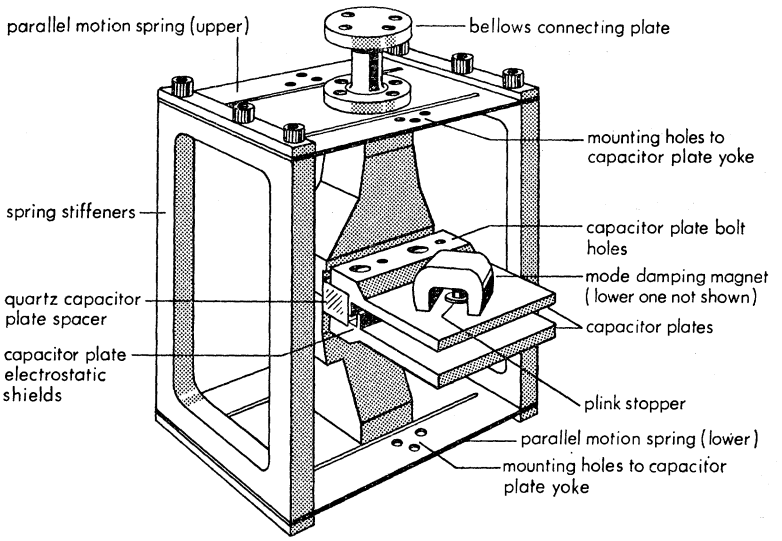

FIGURE 3. Transducer assembly for horizontal and vertical accelerometers. Outer plates of transducer are shown with damping magnets attached. Centre plate is mass in vertical instrument, upper plate of figure 2 in horizontal instrument. Yoke supporting plates rides on parallel motion springs at top and bottom which allow zero adjustment in vertical instrument. Assembly is 11.5 cm in width.

Figure 3 shows the two outer plates of the sensor, separated by a quartz spacer, and the supporting frame, which mates with the frame containing the mechanical system. In the vertical accelerometer (figure 1) the centre plate is the mass itself, while in the horizontal accelerometer the centre plate is a special detector plate mounted above the fibre (figure 2). The geometry of the horizontal instrument was chosen to facilitate the use of the parts originally designed for the vertical; the gain would obviously have been higher had the transducer been built around the pendulum mass, but this loss in gain was easily recovered electronically.

INTERNAL ENVIRONMENTAL CONTROL

Rigid control of both pressure and temperature is inherent in both these instruments. The mechanical system and transducer are mounted in a stainless-steel high-vacuum can sealed with a gold O-ring and evacuated to a pressure of 10^{-5} Pa (10^{-7} Torr). This high-vacuum environment eliminates the effects of convection, variable buoyancy, and humidity. With an outer diameter of 20 cm and a total mass of less than 9 kg, the can and its contents, which constitute the essence of the instrument, are easy to deploy in vaults or boreholes.

Strict stability of the fibre temperature is necessitated by the strong temperature dependence

of the elastic properties of quartz. Although the effect is less important in the horizontal accelerometer, this temperature dependence produces fluctuations of the input to the vertical accelerometer of about 1.2×10^{-4} g/K. To keep the fibre temperature constant, a hybrid system consisting of passive thermal insulation and active thermostatic control is used. The active part of the system is a custom-designed high-gain proportional thermostat using a precision thermistor. Analysis of the output of the vertical accelerometer has shown that the thermal insulation and temperature regulator keep the temperature averaged over the two active fibre sections constant to within 10^{-6} K over 100 s periods and 10^{-5} K over periods of the order of a day.

Filtering and recording of data

The response of the instrument at the output of the phase-sensitive detector used for the position sensor has the shape shown in figure 4. It is essentially the response of the resonant mechanical system, as modified by the low pass filter in the phase-sensitive detector. The basic response is flat over the bandwidth from d.c. to nearly 1 Hz.

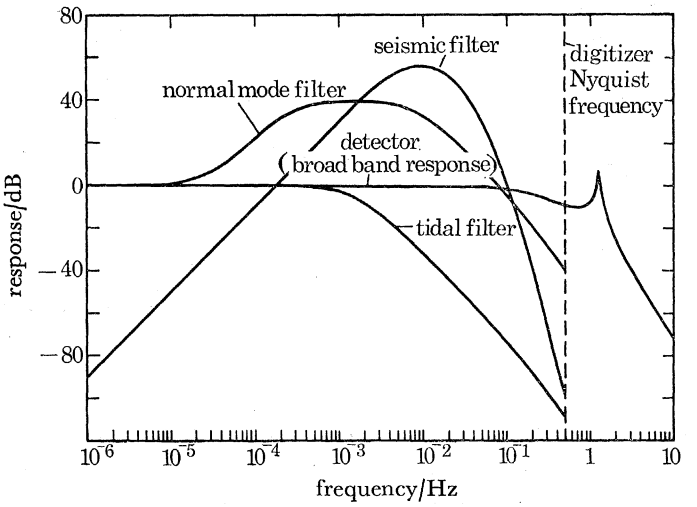

Figure 4. Responses to acceleration at outputs of three analogue filters used for geophysical observations, with broadband response at position sensor output shown for comparison. Broadband response at d.c., here taken as 0 dB, is typically 5×10^6 V/g in amplitude, or about 2×10^{-6} g full scale.

Because the basic response is flat over the entire bandwidth of geophysical interest, active analogue filters (Dratler 1971) are used to observe particular phenomena. Tides are observed with the aid of a double-pole low-pass filter whose cut-off frequency if 5.75 c/h (cycles per hour). Free oscillations of the Earth are recorded at the output of a bandpass filter with a passband from 1 to 30 c/h. The gain of this filter is 40 dB in the passband and unity at d.c. For observation of teleseismic signals, a filter with a response sharply peaked at 100 s periods and half-power points at 60 and 200 s periods is used. The responses at the outputs of the three analogue filters are also shown in figure 4.

All the filter outputs are recorded digitally on magnetic tape at a resolution of 16384 counts per full scale and a sampling interval of 1 s. As shown in figure 4, each active filter provides plenty of attenuation above the digitizer Nyquist frequency (0.5 Hz) to eliminate aliasing. The

large dynamic range of digitization is necessary to take full advantage of the sensitivity and dynamic range of the instrument (Bartholomew, Block & Dratler 1972). All the data shown below are computer plots of either digitized records or the results of analysis.

Phenomena observed

As their names suggest, accelerometers respond to any change in acceleration along the instrumental degree of freedom. Both kinematic acceleration due to motion of the Earth's surface and changes in gravitational acceleration are observed, and the two effects cannot be distinguished on the basis of the instrumental output alone. Motion and tilt of the Earth's surface after earthquakes, direct tidal forces and their effects on the Earth's figure and oceans, tectonic displacement and meteorologically-induced motion of the Earth's surface can all be observed by accelerometers through their kinematic or gravitational effects.

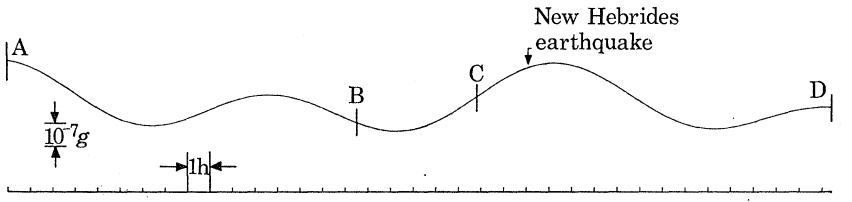

Figure 5. Sample output of tidal filter channel of prototype vertical accelerometer. Record begins at 08 h 29 min 17 s G.M.T. 12 October, 1969 and ends at 20 h 58 min 36 s G.M.T. 13 October. Teleseismic signals from New Hebrides earthquake, shown at higher gain in figure 6, are barely visible due to low gain of tidal channel.

As an example of tidal observations, a record of the tidal filter output of the vertical accelerometer is presented in figure 5. The trace shown is unfiltered raw data; its noise level is not visible on the scale of the plot. Such data from the vertical accelerometer and similar instruments have been analysed in detail by Farrell (1970, 1973).

Free oscillation data

The high sensitivity and broad bandwidth of the quartz fibre accelerometers are used to best advantage in the study of the free oscillations of the Earth. Figure 6 shows the normal mode filter output from the vertical accelerometer for a deep event of surface wave magnitude 6.5 at a great circle distance of 87.1° from the station (Block & Dratler 1971). Relevant source parameters for this and other events discussed in this study are listed in table 1. In the earthquake record, the level of combined ground and instrument noise, or ambient noise, can be seen before the first arrival. The body wave arrivals are seen as sharp spikes due to the condensed time scale, and these are followed by the Rayleigh groups R1 to R4. The earthquake oscillations appear symmetrically superimposed on the tidal signal, showing the broad bandwidth and high linearity of the instrument. Due to the gain and phase response of the normal mode filter, the tidal signals are distorted so that the amplitude scale of the figure does not apply to them.

A spectrum of the 15 h of data of figure 6 is shown in figures 7 and 8. This spectrum is a simple fast-Fourier transform of the data, without smoothing or windowing. For comparison, a similar spectrum of an ambient record of equal length from the previous day, which contained no earthquakes, is plotted in figure 8. The running mean over 1 c/h of this ambient spectrum,

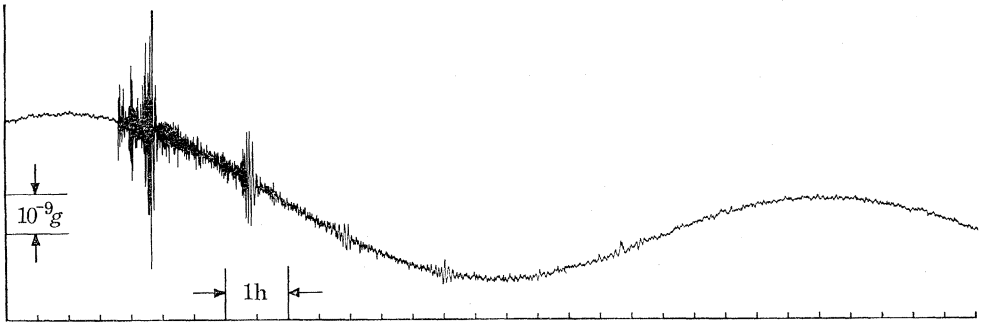

FIGURE 6. Output of normal mode filter of prototype vertical accelerometer for New Hebrides earthquake of 13 Oct. 1969. Record shown corresponds to section CD of tidal data in figure 5. Vertical scale does not apply to tidal signals, which lie outside filter passband and are distorted by phase shifts in filter.

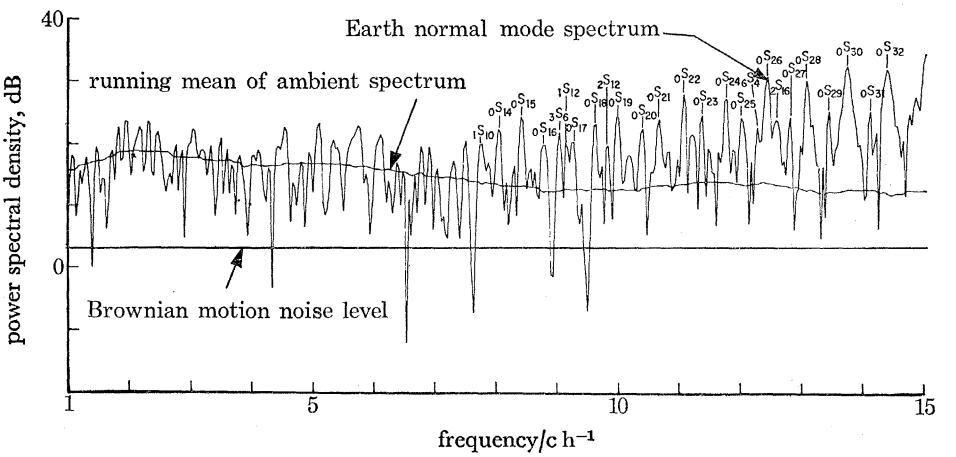

FIGURE 7. Spectra of New Hebrides earthquake record of figure 6 and of ambience (combined ground and instrument noise). Ambient spectrum is derived from normal mode filter data corresponding to section AB of figure 5. Event spectrum shows free oscillation lines identified from theory. Brownian noise level calculated for prototype vertical accelerometer is marked with heavy line. Absolute power spectral density of 0 dB point is $7.4 \times 10^{-25}\ g^2/(\text{c h}^{-1})$. Spectra are not corrected for filter response.

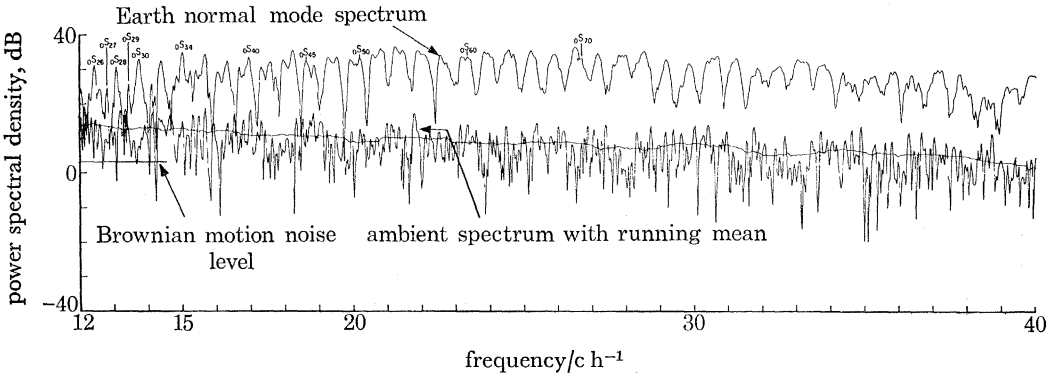

FIGURE 8. Continuation of spectra of figure 7 to higher frequencies, with actual ambient spectrum, as well as running mean, shown for comparison.

including both ground and instrument noise, is shown. The noise and earthquake spectra differ visibly in both character and level, and above 15 c/h the signal-to-noise ratio is greater than 20 dB. Fundamental spheroidal normal modes of the Earth, along with a few overtones, are identified from the eigen-frequency calculations of (Gilbert 1970; Dziewonski & Gilbert 1972). The calculated level of Brownian noise at the input of the vertical accelerometer is indicated by a heavy solid line in the figures.

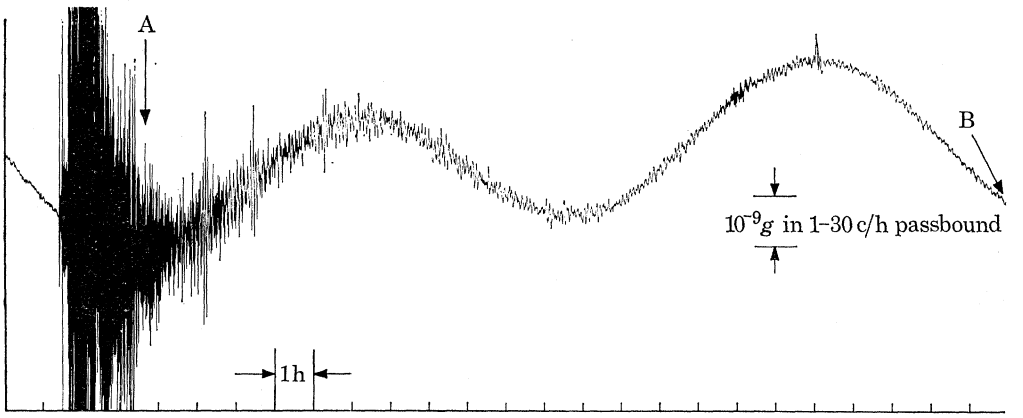

FIGURE 9. Normal mode filter record from prototype vertical accelerometer for Mindanao earthquake of 10 Jan. 1970. Record is clipped due to filter saturation during arrival of large 20 s period Rayleigh waves. Section AB is used for Fourier analysis. Glitch near end of record is due to noise at military base near instrument site. Vertical scale does not apply to tides.

Another example (Dratler 1971; Block & Dratler 1973) of the type of data available from the normal mode filter of the vertical accelerometer is shown in figure 9. This is a record of an earthquake of surface wave magnitude 7.3 at a depth of 73 km and a distance of 107.8° from the station (table 1). The record is similar to that in figure 6 except that the large 20 s period Rayleigh waves have caused saturation of the normal mode filter. After the saturated portion, later Rayleigh group arrivals are visible, and a smaller earthquake and glitch can be seen towards the end of the record. The glitch was due to noise from military airplanes and weapons tests at an air base near the instrument site. Section AB of the record was used for spectral analysis.

Figure 10 shows the spectrum of the 22 h section AB of figure 9. The running mean of the ambient spectrum shown in then the figure was derived from observations nearly 2 months previous to the earthquake, so that the assumption of stationarity of noise implied in this comparison is not entirely sound. Well-defined modal peaks are observed, and certain fundamentals are identified from calculated eigenfrequencies. Records and spectra such as those so far shown are obtained about once a month on the average, with a single vertical accelerometer. This rapid rate of acquisition of data is important for studies of earth models based on free oscillation data (Dziewonski & Gilbert 1972), and for low-frequency investigations of earthquake source mechanisms (Gilbert 1970) (see also the discussion by Gilbert in this volume).

The torsional, or toroidal, modes of free oscillation of the Earth are most easily observed with horizontal accelerometers. Such observations are of interest for comparison with strainmeter recordings, as most operable strainmeters are horizontal. Figure 11 shows an example of the data obtainable at the output of the normal mode filter of the horizontal accelerometer (Dratler 1971; Block & Dratler 1973). The event shown (table 1) is of magnitude $M_S = 7.1$, depth

PHILOSOPHICAL TRANSACTIONS OF THE ROYAL SOCIETY A MATHEMATICAL, PHYSICAL & ENGINEERING SCIENCES

TABLE 1. SOURCE PARAMETERS FOR THE EARTHQUAKES IN THE FIGURES

figure	location and epicentre	Δ1 (deg)	m_b	M_S	$M_S(30°)$	h/km	α[3] (deg)	origin time and date (G.M.T.)	start time and date of record	source[4]
6	New Hebrides, 18.9° S, 169.3° E	87.1	—	6.5	—	246	—	06 h 56 min 01.6 s 13 Oct. 1969	05 h 15 min 53 s 13 Oct. 1969	PDE
9	Mindanao trench 6.8° N, 126.7° E	107.8	—	7.3	—	73	—	12 h 07 min 08.6 s 10 Jan. 1970	10 h 55 min 52 s 10 Jan. 1970	PDE
11	Adak Island, 51.4° N, 177.2° W	46.8	—	7.1	—	43	93.1	06 h 08 min 27.3 s 2 May 1971	06 h 12 min 30 s 2 May 1971	PDE
12	Chile, 25.5° S, 69.2° W	73.8	6.3	—	—	93	90.7	21 h 00 min 40.9 s 17 June 1971	21 h 14 min 50 s 17 June 1971	PDE
14 (event 2)	Tonga trench, 22.8° S, 175.4° W	78	5.0	4.9†	4.2†	33	8	05 h 17 min 58 s 13 April 1971	as shown	LASA
14 (event 3)	Tonga trench, 15.9° S, 174.0° W	73	5.5	4.6†	4.0†	73	13	15 h 57 min 34.5 s 13 April 1971	as shown	PDE
15 (event 7)	Galapagos Island, 2.3° S, 89.6 W	44	4.9	4.6†	4.4†	17	87	05 h 05 min 25 s 19 April 1971	as shown	LASA
16	San Fernando Valley, 34.4° N, 118.4° W	1.9	—	6.5	—	13	—	14 h 00 min 41.6 s 9 Feb. 1971	—	BSSA

Notes: (1) Great circle source-receiver separation calculated from reported epicentre and known location of instrument site (32.88° N, 117.1° W).
(2) Surface wave magnitude of hypothetical event at distance $\Delta = 30°$ which would produce similar record.
(3) Calculated angle between great circle source-receiver path and direction of maximum sensitivity of horizontal accelerometer.
(4) LASA = Bulletin of the Large Aperture Seismic Array, Montana. PDE = Preliminary Determination of Epicentre by National Oceanographic and Atmospheric Administration. BSSA = Seismological Society of America Bulletin, Seismological Notes.

† Surface wave magnitudes calculated from vertical accelerometer records, as shown in Dratler (1971), Block & Datler (1971) and Prothero *et al.* (1971).

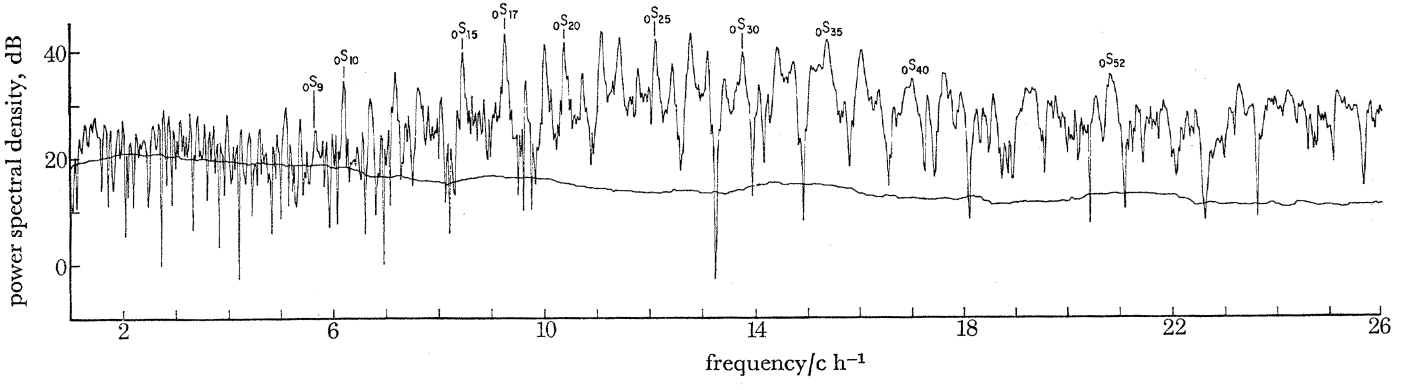

FIGURE 10. Fourier spectrum of section AB of Mindanao earthquake record of figure 9 with running mean of ambient spectrum derived from data taken nearly two months previously. Spectra are not corrected for instrumental response. Normal mode lines are identified from theory.

43 km, and source-receiver distance 46.8°. The source-receiver path was at an angle of nearly 90° to the axis of the horizontal accelerometer (table 1) so that Love waves and the corresponding torsional modes of the Earth were observed. The high level of tilt noise at low frequencies in the surface vault used for these studies is evident.

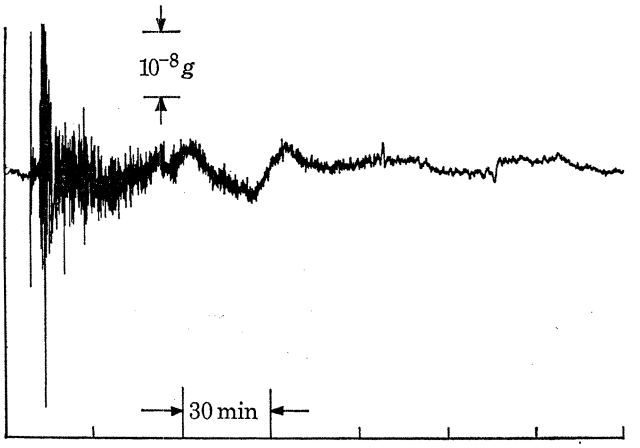

FIGURE 11. Love wave record of Adak earthquake of 2 May 1971, observed through normal mode filter of prototype horizontal accelerometer. Note body wave arrivals early in record and high tilt noise level. Long period wiggle in centre has been observed with other instruments but remains unexplained.

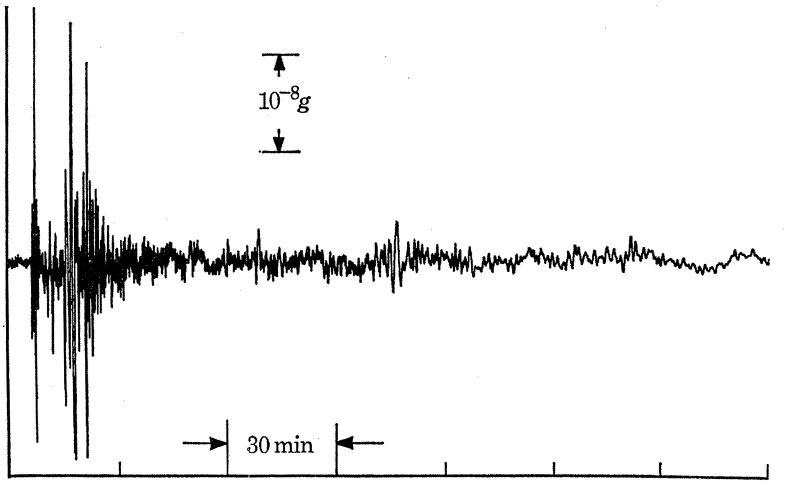

FIGURE 12. Love wave record of Chilean earthquake of 17 June 1971, from normal mode channel of horizontal accelerometer.

An interesting feature of the record of figure 11 is the long period wiggle occurring about 45 min after the first arrival. This same signal was observed with a different instrument at Aberdeen (R. V. Jones, personal communication). Similar signals, low Q oscillations of 15 to 30 min periods, have been observed with the horizontal accelerometer after at least two other events. No explanation of this phenomenon, which follows some earthquakes and not others, is known to the authors.

An example of an earthquake which produced no such long-period wiggle (Dratler 1971; Block & Dratler 1973) is shown in figure 12. For this event, the great circle source-receiver path was again nearly perpendicular to the axis of the horizontal accelerometer, so that Love waves

and toroidal modes were observed. Love wave arrivals G_1 and G_2 are visible in the record, which is otherwise rather unexciting. A Fourier spectrum of the record is shown in figure 13 along with the running mean over 1 c/h of the ambient spectrum taken from a record of the same length. Fundamental toroidal free oscillations of the Earth are observed with nearly a 20 dB signal-to-noise ratio. The horizontal noise level is high in the normal mode band and rises at d.c.

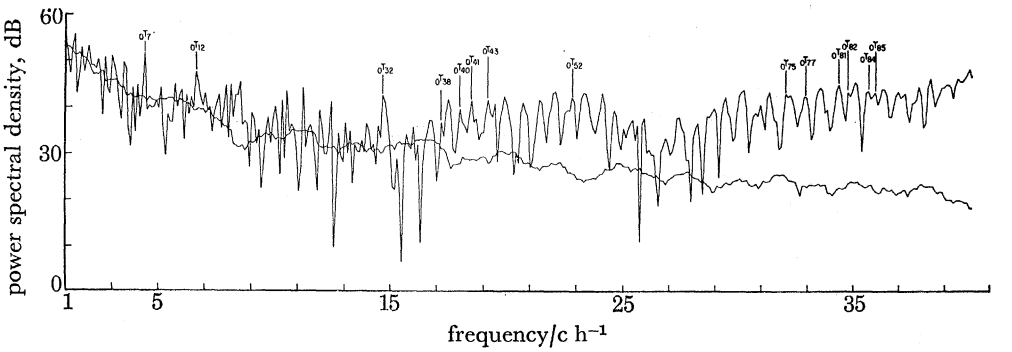

FIGURE 13. Fourier spectrum of 10 h of Chilean earthquake record, of which section in figure 12 is initial part. Running mean of ambient spectrum is derived from data taken about one month previously. Note toroidal modal lines identified from theory and high noise level, increasing near d.c.

SEISMIC DATA

In the domain of teleseismic investigation, the quartz fibre accelerometers have application to the task of detecting small distant events and discriminating between explosions and earthquakes for the purpose of monitoring a ban on underground nuclear tests. For this application, the vertical accelerometer has been found comparable in sensitivity to a bulkier instrument developed specifically for seismic detection, and evaluations of the horizontal instruments are in progress.

At the surface site used for acquisition of preliminary data, horizontal tilt noise in the bandpass of the seismic filter is high (Block & Dratler 1971). However, most of this noise occurs at frequencies slightly below those of teleseismic interest, so that the apparent noise level can be reduced appreciably by digital filtering.

Figure 14 shows the output of the seismic filters for an event of surface wave magnitude 4.9 in the Tonga trench (table 1). The source-receiver path intersected the axis of the horizontal instrument at an angle of only 8°, so that Rayleigh waves were observed with both instruments. The top two traces in the figure are the raw seismic filter outputs for the horizontal and vertical accelerometers respectively. The bottom two traces are the horizontal and vertical data after application of a digital highpass filter which cuts drastically at 45 s periods. The reduction in noise amplitude obtained by digital filtering of the horizontal record is about a factor of 5. Dispersion of the Rayleigh waves is clearly visible on all the traces.

In the records as shown, the horizontal acceleration is underestimated by a factor of 2.2 relative to the vertical, due to a difference in gain between the two instruments. When this factor is taken into account, the polarization ration of the Rayleigh waves, i.e. the ratio of horizontal to vertical equivalent acceleration, is seen to be anomalously high. It is about 2.6 at 20 s periods. This is probably due to the effects of local geology and the nearness of the station to a continental margin.

A similar set of records for a smaller event ($M_S = 4.6$) (table 1) is shown in figure 15. The

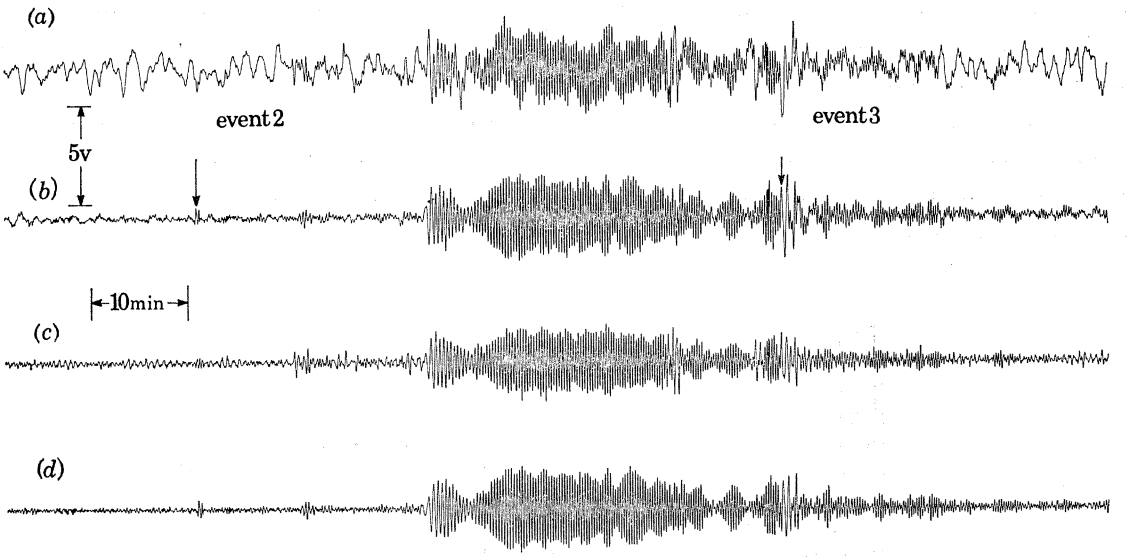

FIGURE 14. Application of records from horizontal and vertical accelerometers to seismic detection problem. Plots show seismic filter data for events 2 and 3 of table 1, both before and after digital filtering. Trace (*a*) is raw horizontal data, while trace (*c*) is horizontal data after application of digital highpass filter with 45 s period cut off. Traces (*b*) and (*d*) are raw and digitally filtered vertical records respectively. In terms of acceleration, horizontal gain for this plot is lower than vertical by factor of 2.2. Note clear Rayleigh wave disperson on all traces and reduction of tilt noise by digital filtering.

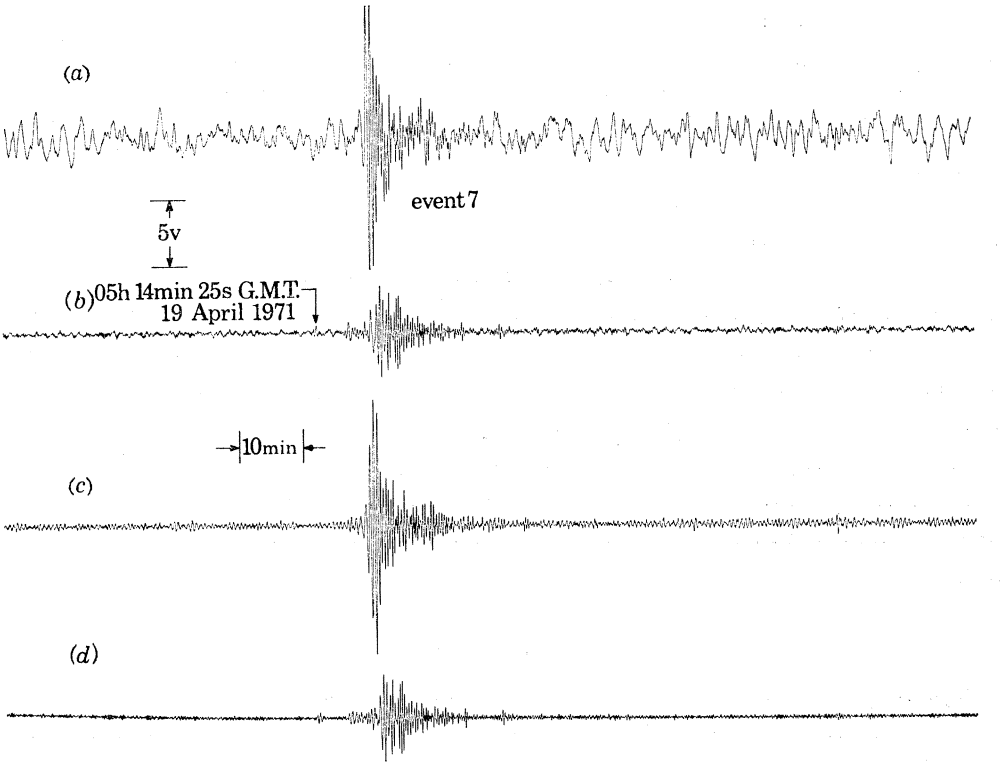

FIGURE 15. Horizontal and vertical seismic filter records as in figure 14 for event 7 of table 1. Rayleigh waves appear on vertical records, Love waves on horizontal. High level of Love wave signals aids in detection and discrimination for distant events.

great circle path for this event was nearly perpendicular to the axis of the horizontal instrument, so Love waves were observed on the horizontal records. The signal-to-noise ratio on the digitally filtered horizontal record is greater than 30, which shows the importance of Love wave observation to the detection problem. Such Love wave records are a valuable discrimination aid, as explosions cannot produce Love waves of the size recorded here. The use of bandpass filtering, rather than highpass filtering, allows detection of a surface wave magnitude 2.5 event at 30° from the vertical records.

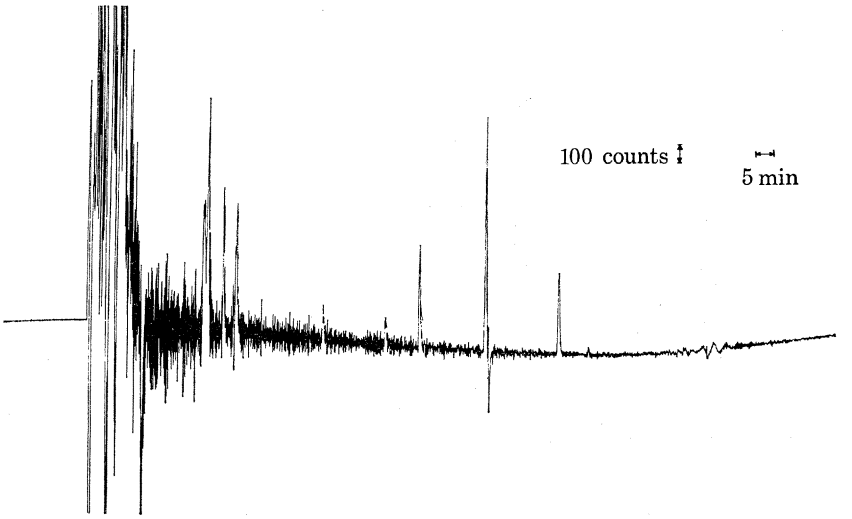

FIGURE 16. San Fernando earthquake of 9 Feb. 1971, observed with vertical accelerometer about 200 km from the epicentre. Owing to high level of signals, main event and aftershocks are clearly observed in tidal channel. Interpolation of d.c. level across saturated portion of main event record yields upper limit for vertical motion of Earth's surface. Vertical scale marked '100 counts' corresponds to about $9 \times 10^{-9}\,g$ in passband of tidal filter (see figure 4).

Certain types of data from the quartz fiber accelerometers can be used for comparison with strain measurements. The record in figure 16 of the well-known San Fernando earthquake of 9 February 1971 (table 1) illustrates this point. Since the normal mode filter channel was saturated due to the proximity of the event to the station, this record is taken from the tidal filter channel. The main event and several after-shocks are clearly visible in the record. By interpolation across the initial saturated portion, and upper bound of $3 \times 10^{-10}\,g$ for a vertical gravity step during the earthquake is obtained. This sets an upper bound of about 1 mm to motion of the Earth's surface relative to the centre of mass of the Earth at a distance of 200 km from the epicentre. Owing to difficulties in interpolation a more stringent upper bound could not be obtained.

CONCLUSIONS

The capability of the new horizontal and vertical quartz fibre accelerometers has been indicated. Due to their stable elastic elements and sensitive transducers, these instruments have broad bandwidth and high gain. Their strictly controlled internal environment and small size and weight make them suitable for borehole deployment and use in arrays. From the viewpoint of strain measurement, they should be useful in measuring siting effects, as accelerometers, which measure at a single point, are less susceptible to siting difficulties than strain meters. So

far, the prototype instruments have provided data of fair interest in the study of tides, free oscillations and earthquake waves. A more comprehensive review of the data is in preparation (Block & Dratler 1973) and further details are available in the references.

The authors would like to thank F. Gilbert for his helpful suggestions on the application of the accelerometers to normal mode studies, J. Brune for his advice on the detection problem, and R. A. Haubrich for suggestions on data analysis.

Particular thanks are due to C. W. Van Sice for his aid in assembling and maintaining the instruments.

References (Block & Dratler)

Bartholomew, B., Block, B. & Dratler, J., Jr. 1972 *Nature Phys. Sci.* **236**, 123–125.
Block, B. & Dratler, J., Jr. 1971 *Nature Phys. Sci.* **232**, 33–37.
Block, B. & Dratler, J., Jr. 1972 *J. geophys. Res.* **77**.
Block, B. & Dratler, J., Jr. 1973 *Rev. Geophys.* (in the Press).
Block, B., Dratler, J., Jr. & Moore, R. D. 1970 *Nature, Lond.* **226**, 343–344.
Block, B. & Moore, R. D. 1970 *J. geophys. Res.* **75**, 1493–1505.
Boys, C. V. 1923 *A dictionary of applied physics* (ed. Sir Richard Glazebrook). London: Macmillan. Vol. III, 695, 1923.
Cavendish, H. 1798 *Phil. Trans. R. Soc. Lond.* **88**, 469.
Derr, J. S. 1969 *Bull seism. Soc. Am.* **59**, 2079–2099.
Dratler, J., Jr. Quartz fiber accelerometers and some geophysical applications. Doctoral thesis, University of California at San Diego, September 1971.
Dratler, J., Jr. & Block, B. 1972 *Geophys. J. R. astr. Soc.* **27**, 337–367.
Dziewonski, A. M. & Gilbert, F. 1972 *Geophys. J. R. astr. Soc.* **27**, 393–413.
Farrell, W. E. Gravity tides. Doctoral thesis, University of California at San Diego, 1970.
Farrell, W. E. 000 *Rev. Geophys.* (to appear).
Gilbert, F. 1970 *Geophys. J. R. astr. Soc.* **22**, 223–226.
Gilbert, F. *Methods of computational physics* (to appear).
Prothero, W., Dratler, J., Jr., Brune, J. & Block, B. 1971 *Nature, Lond.* **231**,
Roll, P. G., Krotkov, R. & Dicke, R. H. 1964 *Ann. Phys.* **26**, 442–517.

PHILOSOPHICAL TRANSACTIONS OF THE ROYAL SOCIETY A MATHEMATICAL, PHYSICAL & ENGINEERING SCIENCES

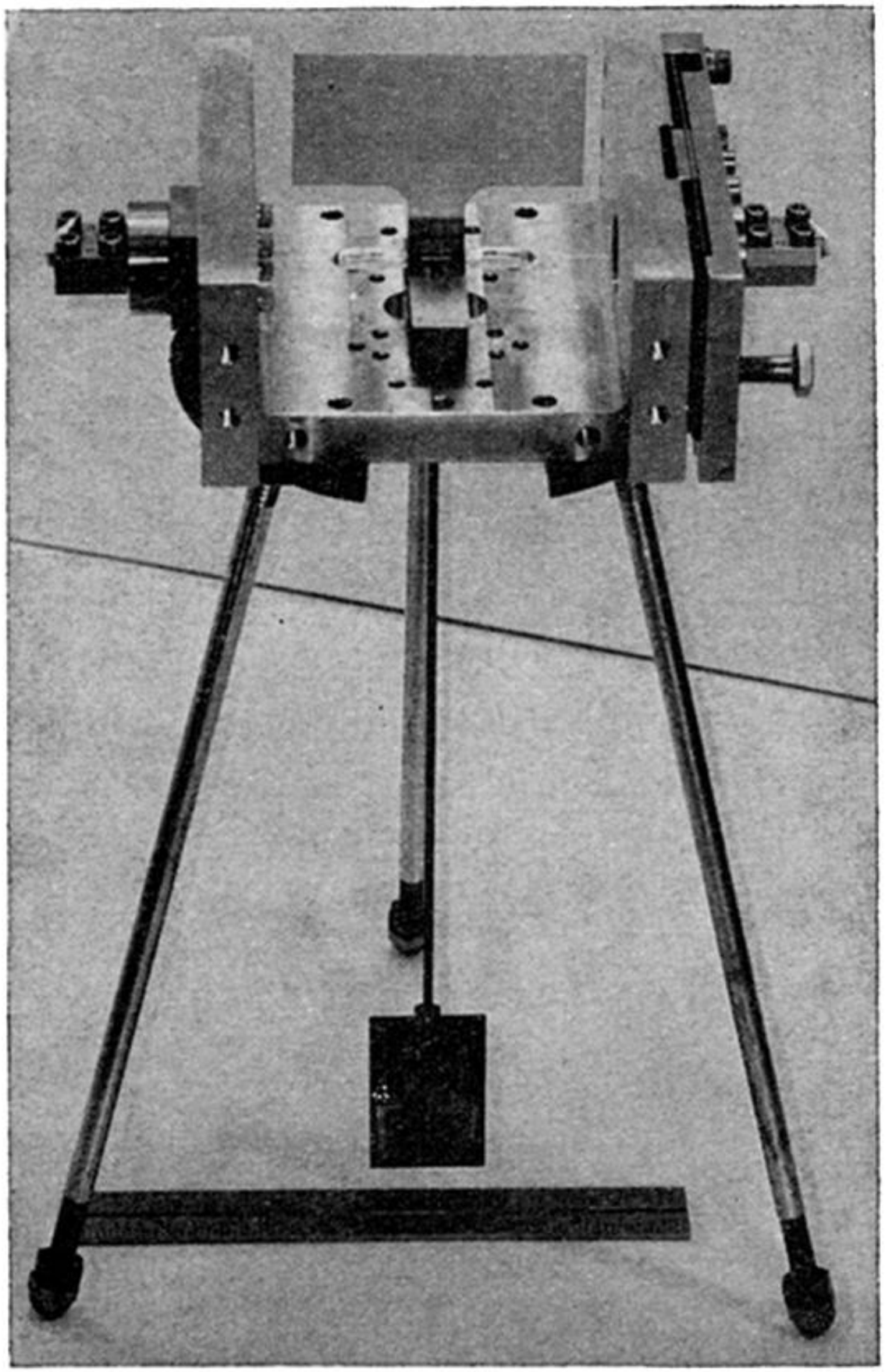

FIGURE 2. Pendulum assembly for horizontal accelerometer. Plate at bottom is pendulum mass. Large plate at top is centre element of transducer, while small fin is used for eddy current damping of unwanted modes of vibration.

PHILOSOPHICAL TRANSACTIONS OF THE ROYAL SOCIETY A MATHEMATICAL, PHYSICAL & ENGINEERING SCIENCES